A Theoretical Approach to Analytical Properties of 2,4-Diamino-5-phenylthiazole in Water Solution. Tautomerism and Dependence on pH

Luis A. Montero,*,† Ana M. Esteva,‡ José Molina,§ Antonio Zapardiel,‖ Lucas Hernández,‖ Heydi Márquez,⊥ and Alexis Acosta⊥

Contribution from the Laboratorio de Química Computacional y Teórica, Departamento de Química Analítica, and Laboratorio de Síntesis Orgánica, Facultad de Química, Universidad de La Habana, Havana 10400, Cuba, Grupo de Modelización y Diseño Molecular, Instituto de Biotecnología, Campus de Fuentenueva, Universidad de Granada, 18071 Granada, España, and Departamento de Química Analítica, Facultad de Ciencias, Universidad Autónoma de Madrid, 28049 Madrid, España

Received April 8, 1998. Revised Manuscript Received July 9, 1998

Abstract: Theoretical models are used to study pH-dependent equilibria of 2,4-diamino-5-phenylthiazole tautomer molecules in water. A complete screening of semiempirical SCF multiple minimums of hypersurfaces, corresponding to several solute−water supermolecules, has been made. Multiple minimum hypersurface searching confirms experimental NMR results indicating that the native diamine tautomer predominates in aqueous neutral and basic media. This tautomeric structure, protonated either in N3 and N4, also predominates in aqueous acid media with a minor presence of a protonated monoimine tautomer, in agreement with ^{1}H NMR results in D$_2$O. High-level ab initio SCF MO of the main structures, where solvent reaction field effects are taken into account with a dielectric constant equivalent to that of water, predict a nonconjugated protonated monoimine tautomer in nonprotic solvents, according to ^{1}H NMR data in polar aprotic solvents. Calculated electron excitation patterns of hydrated species in water agreed with the experimental UV spectra at different pH values. The quantum chemical procedures for calculating total energies and frontier orbital eigenvalues in local minimum geometries of the relevant supermolecules provide an appropriate model for comparisons of theoretical results with experimental facts in the case of analytical voltametry. The frontier orbital eigenvalues of the most populated minimums discard the appearance of electroanalytic signals in the case of acidic samples because of the similarity of the predicted values for all protonated isomers and water. Experimental measurements confirm the oxidative character of electroanalytic signals.

Introduction

Theoretical representations of molecules and their associated processes are usually limited to mostly nonrealistic cases in the gas phase[1] because of the frequent failure to take into account the true effects of the molecular environment. For instance, analytic determinations are normally performed in solution. It is not surprising that in this branch of chemistry theoretical applications are truly scarce. The big effort needed to perform accurate calculations required to obtain more or less confident theoretical images of the several molecules present in real phenomena usually exceeds the availability of computational power. Moreover, the very complex and varying shapes of the significant solute−solvent supermolecules can easily confound the picture.

The most common methods for considering molecular environmental effects are Monte Carlo[2] and molecular dynamic[3] simulations. However, these fail to take into account those collective properties that can only be explained by quantum mechanics, such as bonding effects, because of their use of classical potentials. One way to consider effects on electronic states and bonding is to include them in the calculation of the appropriate Hamiltonians.[4] An alternative approach is to consider the effects of external fields on the "solute" in different ways, as in the procedures pioneered by Tomasi and co-workers,[5] Cramer and Truhlar,[6] or Tapia.[7] In fact, this latter approach was used in a recent attempt to study tautomeric equilibria of hydroxypyridines in different solvents.[8]

The 2,4-diamino-5-phenylthiazole molecule is also known as amiphenazole. It is a drug used as a stimulant in humans and presents a complex structure. Five neutral tautomers are possible: the raw diamine, three monoimines, and one diimine as shown in Figure 1. The compound is shipped for preservation as hydrobromide. If we want to approach all the feasible sites for the first protonation, they might be (i) the sulfur atom in

† Laboratorio de Química Computacional y Téorica, Universidad de La Habana.

‡ Departamento de Química Analítcica, Universidad de La Habana.

§ Universidad de Granada.

‖ Universidad Autónoma de Madrid.

⊥ Laboratorio de Síntesis Orgánica, Universidad de La Habana.

(1) Hehre, W. J.; Radom, L.; Schleyer, P. v. R.; Pople, J. A. Ab Initio Molecular Orbital Theory; J. Wiley & Sons: New York, 1986.

(2) Metropolis, N.; Rosenbluth, A. W.; Rosenbluth, M. N.; Teller, A. H.; Teller, E. *J. Chem. Phys.* **1953**, *21*, 1087.

(3) Jørgensen, W. L. *Acc. Chem. Res*. **1989**, *22*, 184.

(4) Wang, J.; Boyd, R. J.; Laaksonen, A. *J. Chem. Phys*. **1996**, *104*, 7261 and references therein.

(5) Alagona, G.; Ghio, C.; Igual, J.; Tomasi, J. *J. Am. Chem. Soc*. **1989**, *111*, 3417.

(6) Cramer, C. J.; Truhlar, D. G. *Science* **1992**, *256*, 213.

(7) Tapia, O. Solvent Effects on Biomolecules and Reactive Systems. An Overview of the Theory and Applications in *Computational Chemistry, Part A*; Fraga, S., Ed.; Elsevier: Amsterdam, 1992; p 694.

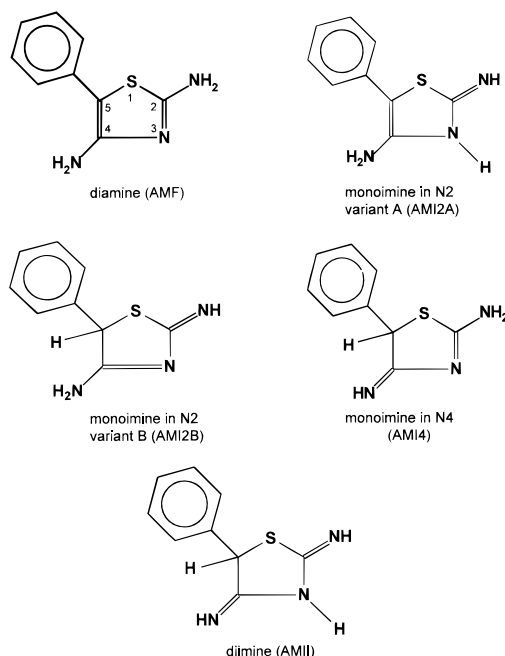(8) Wang, J.; Boyd, R. J. *J. Phys. Chem.* **1996**, *100*, 16141.

Figure 1. Isomeric structures of 2,4-diamino-5-phenylthiazole.

the ring (S1), (ii) the nitrogen atom attached to the α-carbon atom (N2), (iii) the nitrogen atom in the ring (N3), and (iv) the nitrogen atom attached to the γ-carbon atom (N4). During preparative and analytical processes, this substance may appear as a neutral species in aprotic solvents or very dilute water solutions at pH values higher than 8. However, all water solutions containing a significant concentration of amiphenazole must have a lower pH, and consequently, the species must be protonated at least once.[9]

NMR experimental results[10] to decide the most abundant isomers are not conclusive but indicative. In the case of amiphenazole hydrobromide, the ^{1}H NMR spectrum in heavy water solution only shows a small and doubtful nonaromatic proton signal that is noisy and hardly integrates to a single proton. This small peak must correspond to a certain population of C5 saturated isomers. Amine- or imine-type protons give nonobservable signals in heavy water because of their exchange with the solvent. Therefore, the most important isomers of the protonated molecule in water must be either AMF or AMI2A. ^{13}C NMR spectra in aqueous media manifest confusing results concerning the site of protonation, with the only constraint being that it must occur either on N3 or N4.

Changing to a polar aprotic solvent, such as deuterated dimethyl sulfoxide, also changes the pattern of the ^{1}H NMR spectrum of amiphenazole hydrobromide. Now appears a form with a proton on the C5 site of the thiazole ring. This is evidence of AMI2B, AMI4, or AMII as the most favored protonated tautomer in that solvent. Therefore, the experimental facts of the protonated molecules confer to the protic character of the solvent an influence on the type of conjugation between the two rings.

On the other hand, neutral amiphenazole in deuterated water shows no ^{1}H NMR signal of a proton on C5. Therefore, it must correspond to either the diamine AMF or the monoimine AMI2A. The point is that we are facing a complex problem where hydration, protonation, and isomerization are all playing important roles.

(9) Esteva, A. M.; Zapardiel, A.; Bermejo, E.; Hernández, L., to be published.
(10) Pérez, C. S.; del Bosque, J. R.; Rodríguez, Y.; Márquez, H., Acosta, A., to be published.

The main challenges for building a theoretical representation of amiphenazole behavior in solution are three overlapping features: (i) the complex tautomeric equilibria of five different isomers, as described above (see Figure 1); (ii) the four Lewis base sites in each isomer; (iii) the eventual conjugation between π-electron clouds of the phenyl and thiazole rings, which depends on the torsion angle around the common C−C bond of each isomer and which influences the UV−visible spectra.
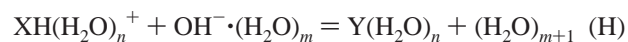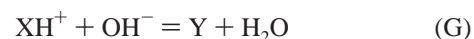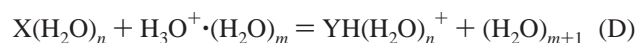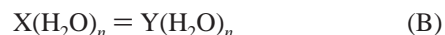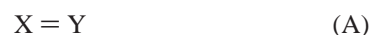
The first purpose of this paper is to build a theoretical picture of the most favored structures in equilibria, for either the neutral or the protonated species. A theoretical approach must take into account the structures of the molecules involved and the effects of the solvent and the pH on them. According to the previous discussion, calculations are made at a high level of theory for the neutral and the most probable protonated species of 2,4-diamino-5-phenylthiazole, where solvent effects are included when the continuum model is used.

Moreover, the theoretical hypersurfaces corresponding to all neutral tautomers and their possible cations, and their association with water molecules, are also explored. This is done by means of approximate quantum mechanical Hamiltonians and their gradient pathway calculations down to local minimums corresponding to different supermolecular geometries. Thus, the most important arrangements of solute−solvent cells corresponding to these local minima are treated by statistical thermodynamical formulas to estimate association energies and entropies.

The solute−solvent cells of the most favored supermolecular structures are then used for calculations of the expected UV−visible spectra, depending on the pH in water, to obtain a theoretical simulation of molecular environmental effects on this physical property. Finally, the preferences of the electroanalytic behavior for hydrated species as carriers of charge are obtained after the appropriate analysis of the MO patterns and the effects of water on them.

Nature of the System under Study

To approach the problem, several reactions can be taken into account to cover the chemical behavior of this system either in the gas phase or in an aqueous media:

$$X = Y \tag{A}$$

$$X(H_2O)_n = Y(H_2O)_n \tag{B}$$

$$X + H_3O^+ = YH^+ + H_2O \tag{C}$$

$$X(H_2O)_n + H_3O^+ \cdot (H_2O)_m = YH(H_2O)_n^+ + (H_2O)_{m+1} \tag{D}$$

$$XH^+ = YH^+ \tag{E}$$

$$XH(H_2O)_n^+ = YH(H_2O)_n^+ \tag{F}$$

$$XH^+ + OH^- = Y + H_2O \tag{G}$$

$$XH(H_2O)_n^+ + OH^- \cdot (H_2O)_m = Y(H_2O)_n + (H_2O)_{m+1} \tag{H}$$

where X and Y can be, indiscriminately, AMF, AMI2A, AMI2B, AMI4, or AMII (see Figure 1).

Reactions A and B consist of tautomerizations in neutral or basic media. They are only significant if X and Y are different. Reactions C and D are protonations of neutral species and their possible tautomerizations. Reactions E and F consist of tautomerizations in acidic media. Reactions G and H are neutral-

izations, including also the possibility of tautomerization. The even-numbered reactions correspond to processes in water solution.

To simulate equilibria in different media, the selected computational model must regard all these reactions. Five isomers with four protonation sites each require a considerable amount of calculation since in order for our final results to be statistically significant several cells must be considered (see below). Reactions A and B imply 10 possibilities. Each of reactions C, D, G, and H requires 100, and reactions E and F require that *380* possibilities must be considered.

Theory and Procedures

The theoretical models of this work need to take into account solvent effects to approach the expected behavior of all the above equilibria. We have used two different approaches, which are guided by two main criteria: first, the huge amount of calculations necessary to account for five isomers and four protonation sites and, second, the capacity to reproduce true solvent effects. These may originate both as a polarity in the environment and by direct interaction among solute and solvent molecules.

Calculations where the solvent effects are approached from the point of view of a field due to the molecular environment were performed at a sophisticated theoretical level by means of ab initio SCF MO[11] calculations including correlation energy[12] and solvent effect corrections.[13]

We must look for a straightforward way to include the corrections due to environmental effects in the usual isolated molecule calculations. Since we are working with chemical transformations and equilibria, some useful relationships can be obtained. For a simple change in an isolated molecule:

$$X = Y \qquad (1)$$

$$\Delta\Omega^{isol} = \Delta\Omega_Y - \Delta\Omega_X \qquad (2)$$

where Ω is any intensive thermodynamic quantity, like enthalpy *H*, free energy *G*, or entropy *S*.

The process for association between a solute and solvent molecules can be described by

$$X + n\text{solvent} = X(\text{solvent})_n \qquad (3)$$

and, in such case the change in the corresponding to thermodynamic quantity is

$$\Delta\Omega_X^{assoc} = \Delta\Omega_{X(solvent)n} - \Delta\Omega_X - n\Delta\Omega_{solvent} \qquad (4)$$

If a given reaction occurs while association between solute and solvent is present, as in a real system, we have (eq B)

$$X(\text{solvent})_n = Y(\text{solvent})_n \qquad (5)$$

We can write, by working with eq 4

$$\Delta\Omega° = (\Delta\Omega_Y^{assoc} + \Delta\Omega_Y + n\Delta\Omega_{solvent}) - $$
$$(\Delta\Omega_X^{assoc} + \Delta\Omega_X + n\Delta\Omega_{solvent}) \qquad (6)$$

Then, the standard properties of the given reaction can be obtained from the values for the isolated conditions including

a correction consisting of the calculated values for the association process. Thus,

$$\Delta\Omega° = \Delta\Omega_Y - \Delta\Omega_X + \Delta\Omega_Y^{assoc} - \Delta\Omega_X^{assoc} \qquad (7)$$

or

$$\Delta\Omega° = \Delta\Omega^{isol} + \Delta\Omega^{assoc} \qquad (8)$$

Therefore, the standard property can be expressed as a sum of the difference of the property between the isolated Y and X solutes plus its difference for their respective solvation reactions. This partitioning simplifies greatly the understanding of the solvation influence in any process by means of $\Delta\Omega^{assoc}$, which can be used as a correction to the usually calculated energy of the states of the isolated molecules by quantum chemical methods. Let us describe now an appropriate way to approach it.

To take into account both the field and the molecular exchange in solute−solvent interactions, we tried a simple statistical approach, as follows. Let us consider a canonical ensemble composed of *M* cells or supermolecules, X(solvent)_*n*, at constant temperature and volume. The supermolecule formation is eq 3 above.

The energy, of the *i*th cell in the *k*th state of the ensemble may be obtained by solving the appropriate Schrödinger equation. *Our attention will focus on finding a reduced set of cells that can represent the most significant contributions to the* k*th state for the whole system.* Then, we will use the Boltzmann distribution to calculate the thermally averaged state of the typical macroscopic system at room temperature.

In statistical terms,[14] the internal energy, entropy, and Helmholtz free energy of molecules can be expressed, respectively, as

$$E = RT^2\left(\frac{\partial \ln q}{\partial T}\right)_V = RT^2\frac{q'}{q} \qquad (9)$$

$$S = R \ln q + E/T \qquad (10)$$

$$A = -RT \ln q \qquad (11)$$

where *q* is the *molecular partition function*, i.e., the statistically weighted sum of states corresponding to the given ensemble

$$q = \sum_i g_i e^{-\epsilon_i/RT} \qquad (12)$$

In any case, the partition function of eq 12 should be calculated by assuming the appropriate energy scale with respect to a reference value. For this purpose, a conventional state has to be chosen for calculating such reference energy. For instance, *we can define such a state to exclude all interaction energies among constituent molecules in a given supermolecule.* This means that we would consider the translational, rotational, and vibrational states of molecules in the supermolecules as identical to those in the reference states. The association process is considered to be isothermal. In this case, the reference state is taken as a set with the same number of noninteracting molecules of the same kind, so that the sum of their total energies is taken as the reference value on our energy scale. Thus, in the reference state $q = 1$. Accordingly, the cell energy with respect to the new reference scale, $\Delta\epsilon_i$, is

(11) Roothaan, C. C. *J. Rev. Mod. Phys.* **1951**, *23*, 69.
(12) Møller, C.; Plesset, M. S. *Phys. Rev.* **1934**, *46*, 618.
(13) Miertus, S.; Tomasi, J. *Chem. Phys.* **1982**, *65*, 239. (b) Miertus, S.; Scrocco, E.; Tomasi , J. *Chem. Phys.* **1981**, *55*, 117.

(14) Matvéev, A. N. *Física Molecular*; Mir: Moscow, 1987; p 227.

$$\Delta\epsilon_i = \epsilon_i - \epsilon^{\text{ref}} \tag{13}$$

where

$$\epsilon^{\text{ref}} = \epsilon_{\text{tot(X)}} + n\epsilon_{\text{tot(H}_2\text{O)}} \tag{14}$$

Consequently, the molecular partition function in the new reference scale is

$$q^* = \sum_i g_i e^{-(\Delta\epsilon_i/RT)} = q e^{\epsilon^{\text{ref}}/RT} \tag{15}$$

By working with eqs 13, 9−11, and the new partition function in eq 15,

$$E^{\text{assoc}} = E - E^{\text{ref}} = RT^2(q^{*\prime}/q^*) \tag{16}$$

$$S^{\text{assoc}} = S - S^{\text{ref}} = R \ln q^* + E^{\text{assoc}}/T \tag{17}$$

$$A^{\text{assoc}} = A - A^{\text{ref}} = -RT \ln q^* \tag{18}$$

To compare the experimental enthalpy and Gibbs free energy values, defined at constant pressure, with the calculated association energies, we can introduce ideal gas corrections. Then, $E^{\text{assoc}} = H^{\text{assoc}} + \Delta nRT$, and consequently

$$H^{\text{assoc}} = RT^2(q^{*\prime}/q^*) - \Delta nRT \tag{19}$$

$$G^{\text{assoc}} = -RT \ln q^* - \Delta nRT \tag{20}$$

According eq 8, the ΔnRT term cancels when we are dealing with chemical reactions and consequently $\Delta H^{\text{assoc}} = \Delta E^{\text{assoc}}$ and $\Delta G^{\text{assoc}} = \Delta A^{\text{assoc}}$ in such cases.

It must be pointed out that the association process described by eq 3 implies the appearance of nonnegligible values of energy corresponding to certain intermolecular degrees of freedom related to the solute−solvent supermolecule. They are those related to the rotational modes of the cluster and the $3(n + 1)$ − 6 *intermolecular* modes of vibration. It can be considered that the neglect of these thermal contributions to the association energy terms above will not be important since their expected significance must be small with respect to the principal energy values. Moreover, in all cases of hydrated transformations B, D, F, and H, such values must tend to cancel for they would appear on both sides of the chemical equations, and what differences might remain are insignificant.

We now focus on how to obtain the energy term. It is noteworthy that the arrangement of a supermolecule with energy can be considered as one local minimum i in its hypersurface, which has several wells depending on nuclear and electronic coordinates. If we take an arbitrary arrangement of molecules as the starting point, traditional gradient minimization procedures[15] with respect to the supermolecular Hamiltonian will arrive to a local minimum that could be statistically significant for the kth ensemble state. It is thus advisable to explore the *multiple minimums hypersurface* (MMH) of supermolecular system by generating several sets with initial random geometries and following a gradient pathway to search for the respective well toward which each arrives.

We note that in following a gradient path to find such minimums, the corresponding Hamiltonians and energy derivatives on each atom in every cycle of optimization for thousands of molecular arrangements must be obtained. This gives a

significant statistical weight to the final and selected local minimum cells to be included in a valid partition function. Thus, an appropriate collection of supermolecules obtained in this way, as well as their respective energies and geometries, must represent a set of the most important states that are significant to the thermodynamic properties of the whole system.

The calculation of the total energy, ϵ_i, corresponding to the ith cell that includes the appropriate number of water molecules, is a very big job in the current state of quantum chemical methods. If ordinary ab initio SCF procedures are used, some important and mutually related problems arise. First is the huge computational effort required to calculate the total energies of cells having a sufficient amount of molecules to meet the previous requirements. Second, there is the great importance of correlation effects when dealing with the long-range interaction energy among separate molecules in each cell. Third, there is the basis set superposition error (BSSE) which usually tends to overestimate molecular interactions in an erratic way. Finally, we have the previously unpredictable and possibly very large number of calculations for different cells needed to select those representing a given state. Some previous calculations of water clusters with high-level ab initio SCF-MO basis set corroborate these considerations.[16]

A plausible alternative for the calculations of supermolecules in the manner of serial procedures is the use of a semiempirical Hamiltonian. An important disadvantage of this approach due to the lack of formalistic rigor must be recognized in the unpredictable accuracy of single calculations. However, such calculations present important advantages for this case: (i) computations are much faster in the case of large supermolecules; (ii) correlation effects are implicitly considered during the parametrization procedures with respect to experimental values[17] (similar arguments justify the recently popular DFT approximations); (iii) BSSE cannot appear because of the orthogonality of atomic orbital basis set; and (iv) long-range interactions between atoms are implicit both in the atomic terms of the Hamiltonian and in the core−core interaction corrections because large molecules, when they are present, are included as references during the parametrization process.

Accordingly, we have chosen a semiempirical SCF-MO Hamiltonian,[18] after some empirical corrections, to improve the results of hydrogen bond and other long-range interactions.[19] The so-called MNDO-PM3 method[20] has been parametrized using the standard heats of formation of a large set of typical reference molecules. It has been designed to reproduce standard heats of formation from total energies (after the inclusion of accurate experimental atomization heats) in the case of molecular geometries corresponding to the minimal SCF value of trial molecules, among other properties. This method reproduces the hydrogen-bonding patterns between water molecules.[21]

All MO and energy gradient calculations in this work have been performed with the MOPAC program.[22] The minimization method selected was the so-called *eigenvector following* (EF),[15,23] which has been designed to search for critical final structures,

(15) Culot, P.; Dive, G.; Nguyen, V. N.; Ghuysen, J. M. *Theor. Chim. Acta* **1992**, *82*, 189.

(16) Jensen, J. O.; Krishnan, P. N.; Burke, L. A. *Chem. Phys. Lett.* **1995**, *246*, 13.

(17) Dewar, M. J. S. *J. Phys. Chem.* **1985**, *89*, 2145.

(18) Dewar, M. J. S.; Thiel, W. *J. Am. Chem. Soc.* **1977**, *99*, 4907.

(19) Dewar, M. J. S.; Zoebisch, E. G.; Healy, E. F.; Stewart, J. J. P. *J. Am. Chem. Soc.* **1985**, *107*, 3902.

(20) Stewart, J. J. P. *Comput. Chem.* **1989**, *10*, 209.

(21) Stewart, J. J. P. *J. Comput. Chem.* **1989**, *10*, 221.

(22) Stewart, J. J. P. MOPAC, v. 6, release for PC computers by L.A.M. in the Laboratory of Computational and Theoretical Chemistry, Universidad de La Habana, 1993−1997, and v. 7, for Linux system as implemented in the same laboratory, 1995.

(23) Baker, J. *J. Comput. Chem.* **1986**, *7*, 385.

as transition states. It is supposed to be a more confident by avoiding sudden molecular rearrangements in the final steps of the minimization path due to any possible overestimation of geometry changes when the molecules are too close together. In fact, this very common problem of MOPAC optimization of nonstandard structures, with the keyword *precise*, was avoided in all of the calculations performed.

A series of 15 or more sets with the solute surrounded by randomly arranged water molecules was generated for each solute species and then optimized, and the results were processed. Normally, E^{assoc} attained a stationary value around the 10th or earlier cell. However, in certain cases, when ΔAassoc was particularly sensitive, up to 45 sets were generated and optimized. Independent calculations of selected cases with the same number of sets converged to thermodynamic quantities with no significant differences. It demonstrates the consistency of this procedure.

The program for generating random sets was specially written for this type of work. It is called GRANADA[24] and inputs molecular set data, such as the radius of distribution around the coordinate origin in the solute molecule and the number of solvent molecules to be taken into account. It outputs the desired series of different arrangements of solute and solvent molecules as input files for MOPAC. Each solvent molecule is situated in a randomly selected new center of coordinates with respect to the solute and is rotated, also randomly, around the three coordinate axes. All cases where the newly generated molecules overlap the van der Waals volume of any existing molecule are discarded. Seeds for the random number generating routines were taken for each new molecular set from the product of the seconds and the hundredths of seconds of the computer clock when the program begins each calculation, to avoid any equivalent random number series. Randomness has been carefully tested.

Thus, the final energy of a significant cell is obtained after navigation in the $3N - 6$ dimensional space of atomic coordinates in each set, where N is the total number of atoms, departing from a random arrangement of all molecular subsystems and arriving at a conventional local minimum. The driving vector for such navigation is provided by the corresponding $3N - 6$ gradients of the total energy corresponding to each SCF cycle over all bodies considered in the set. Hundreds of thousands of SCF cycles, with their respective supermolecular geometries, were calculated during the process for each set. This is a good basis for the statistical quality of our considerations, as we pointed out above. The program for processing the output data is called Q1.

This procedure has been previously tested with water clusters,[25] the case of chemical reaction mechanisms,[26] and the effects of solvents on excited states of organic molecules.[27]

UV spectra of significant supermolecules have been calculated by the NDOL procedure[28] using the corresponding program released by the Havana's laboratory.[29] This method improves the approximate NDO Hamiltonian[30] and is able to take into

account differences between σ and π contributions to the MO energies. Configuration interaction (CI) of the 75 lowest energy SCF singly excited electronic states gives theoretical UV spectra. The corresponding graphics shown in this paper take the oscillator strength, *f*, of each maximum as a measure of the intensity, or probability, corresponding to each electronic transition. The oscillator strength is normally understood as being proportional to the area under the curve of the observed molar absorptivity vs wavenumber.[31] It must be pointed out that a rigorous comparison between experimental and theoretical results can only be performed when the abscissas are expressed in wavenumbers or any other magnitude that is proportional to energy and ordinates in terms of molar absorptivity. However, the analytical chemistry practice imposes the use of wavelengths λ (in nm) and absorbance for abscissas and ordinates, respectively, and we follow this convention in the present paper when comparing spectra, although all calculations for fitting the curves are made by employing the appropriate units. ZINDO/S[32] calculations were also performed for comparisons in the case of UV spectra as implemented in the Hyperchem package of programs (version 3).

The ab initio SCF calculations have been performed by Gaussian 94.[33] Geometries were optimized at the 4-31G** level and single-point 6-311G**, 6-311G**-MP2, and 6-311G**-SCRF energies with the PCM model were then calculated. Due to the large amount of basis functions originated by this molecule, a test of full optimization has been only made in four cases at the 6-311G** level. Differences with respect to the corresponding geometry optimizations at the 4-31G** level amounted only to fractions of kilojoules per mole in all cases of equilibria and were nonsignificant for our conclusions.

Results and Discussion

The first step was to explore the physicochemical hypersurface of the five tautomers with four different protonation sites by the procedure described above using eqs 16 and 18.

(a) Hydration Shell. The first step was dedicated to establishing the amount of water molecules to be considered in a single solute−solvent cell to account for the most significant effects. The AMF diamine was used for this purpose and the amount of water molecules was incremented sequentially to reach a minimal value of E^{assoc}/mol of solvent (see Table 1). It occurred with four water molecules in the case of the neutral diamine and only with one or two water molecules in the case of the site polarized ionic species.

Figure 2 shows the evolution of E^{assoc}/mol of solvent corresponding to hydration shells with a increasing number of water molecules. It has been built by taking into account all optimized sets up to 15. Two important features can be easily recognized: (a) the lowest energy values correspond to the four water molecule solvation shell, as mentioned above, and (b)

(24) Available on request.

(25) Montero, L. A.; Llano, J.; Molina Molina, J.; Fabian, J., to be published.

(26) Rosquete, G. A.; Llano, J.; Álvarez-Idaboy, J. R.; Montero, L. A., to be published.

(27) Mora, N.; Montero, L. A.; Fabian, J. *J. Mol. Struct. (THEOCHEM)* **1998**, *453*, 45.
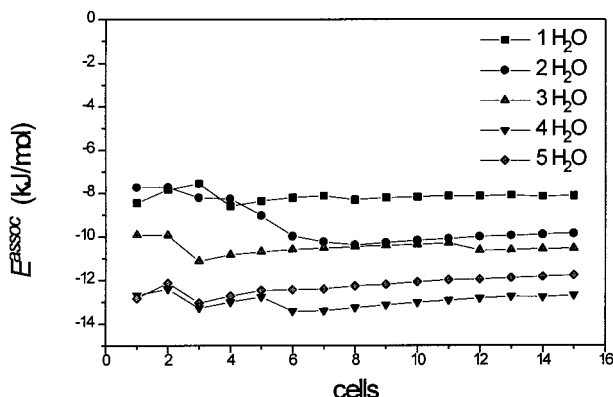
(28) Montero, L. A.; Alfonso, L.; Alvarez, J. R.; Pérez, E. *Int. J. Quantum Chem.* **1990**, *37*, 465.

(29) Montero-Cabrera, L. A.; Alvarez-Idaboy, J. R.; Del Bosque-Arin, J. R.; Cano, R.; González, M. C.; Rodríguez-Montero, M. d. C. *FCTL, Folia Chim. Theor. Latina* **1988**, *16*, 33. Version 3.0, for 200 atoms and 500 basis functions, 1995.

(30) Pople, J. A.; Beveridge, D. L. *Approximate Molecular Orbital Theory*; McGraw-Hill: New York, 1970.

(31) Herzberg, G. *Molecular Spectra and Molecular Structure. I. Spectra of Diatomic Molecules*; Van Nostrand Reinhold Co.: New York, 1950; p 383.

(32) Ridley, J. E.; Zerner, M. C. *Theor. Chim. Acta* **1973**, *32*, 111. Bacon, A.; Zerner, M. C. *Theor. Chim. Acta* **1979**, *53*, 21.

(33) Frisch, M. J.; Trucks, G. W.; Schlegel, H. B.; Gill, P. M. W.; Johnson, B. G.; Robb, M. A.; Cheeseman, J. R.; Keith, T.; Petersson, G. A.; Montgomery, J. A.; Raghavachari, K.; Al-Laham, M. A.; Zakrzewski, V. G.; Ortiz, J. V.; Foresman, J. B.; Cioslowski, J.; Stefanov, B. B.; Nanayakkara, A.; Challacombe, M.; Peng, C. Y.; Ayala, P. Y.; Chen, W.; Wong, M. W.; Andres, J. L.; Replogle, E. S.; Gomperts, R.; Martin, R. L.; Fox, D. J.; Binkley, J. S.; Defrees, D. J.; Baker, J.; Stewart, J. P.; Head-Gordon, M.; Gonzalez, C.; Pople, J. A. *Gaussian 94*, Revision E.2, Gaussian, Inc.: Pittsburgh, PA, 1995.

12028   *J. Am. Chem. Soc., Vol. 120, No. 46, 1998*

Montero et al.

Table 1. Association Energy per Mole of Water with Respect to the Number of Water Molecules in the Case of AMF[a]

no. of H₂O molecules	$-E^{assoc}$				
	neutral	S1	N2	N3	N4
1	8.3	35.4	42.7	42.7	46.0
2	10.5	35.4	44.6	32.9	39.7
3	11.8	32.1	33.4	34.5	36.8
4	14.3	27.0	32.7	32.2	34.5
5	13.5	25.3	26.5	29.4	31.9

[a] Energies (in kJ/mol) of H₂O. S1, N2, N3, and N4 indicates the protonated form in the corresponding site of tiazole ring.

Figure 2. Association energies of AMF with increasing degrees of hydration.

Table 2. Solvation Energies of Neutral Molecules[a]

	X·(H₂O)₅		
X	E^{assoc}	A^{assoc}	$\Delta E^{solv b}$
AMF	−67.6	−69.6	−51.5
AMI2A	−67.9	−71.0	−62.4
AMI2B	−78.8	−82.9	−95.9
AMI4	−72.2	−75.9	−98.2
AMII	−65.7	−68.1	−42.9
H₃O⁺	−353.4	−357.4	−403.3
H₂O	−17.1	−21.5	−31.2

[a] All energies in kJ/mol. [b] Energy of solvation according the Tomasi's SCRF (dielectric constant of water) at 6-311G** level (see text).

the trend to stabilize E^{assoc} values since the 12th cell, approximately, in all cases.

As the same amount of water molecules must be normalized for all other tautomers and their respective protonated forms in order to preserve the stoichiometry of equilibria, the choice of five water molecule solvation shells in all cells was preferred.

It must be stated that in order to obtain a full representation of solvent effects on the solute, a larger number of solvent molecules is needed. Perhaps, the best cluster is attained when the association energy per solvent molecule converges to a certain value. However, as our purpose is to take into account the main effects of the environmental molecules on the solute physical and chemical properties, this relatively small solvation shell of five water molecules should represent the main perturbations to these properties with respect to the isolated solute. In this case, the "solvent solvation" energy appearing after the point when E^{assoc} per water molecule begins to rise again becomes an undesirable and costly effect.

(b) Equilibria of Neutral Species. Association energies, as described in eqs 16 and 18, and solvation energies from Tomasi's self-consistent reaction field calculations at the 6-311G** level, are shown in Table 2. The most suitable values for stabilization are those of nonconjugated monoimines AMI2B

Table 3. Calculated Energies of Tautomerization for Neutral Species[a]

	$\Delta H^{\circ b}$ (anh)	$\Delta H^{\circ c}$	$\Delta G^{\circ c}$	$\Delta H^{\circ b}$ (anh)	$\Delta E^{\circ e}$ (solv)
AMF = AMI2A	17.6	17.3	16.2	48.1	37.2
AMF = AMI2B	49.0	37.8	35.6	15.9	−28.5
AMF = AMI4	55.1	50.5	48.8	27.7	19.0
AMF = AMII	42.5	44.4	44.0	24.5	−18.4
AMI2A = AMI2B	31.4	20.5	19.4	−32.2	−65.7
AMI2A = AMI4	37.5	33.2	32.6	−20.3	−56.2
AMI2A = AMII	24.9	27.1	27.8	−23.6	−55.6
AMI2B = AMI4	6.1	12.7	13.2	11.8	9.5
AMI2B = AMII	−6.5	6.6	8.4	8.6	10.1
AMI4 = AMII	−12.6	−6.1	−4.8	−3.2	0.6

[a] All energies in kJ/mol. [b] Direct calculation from the output heats of formation after the MNDO-PM3 optimization of isolated molecules. Corresponds with reaction A for ΔH° (anh). [c] Calculated by the MMH procedure according to reaction B with water molecules ($n = 5$). [d] HF SCF 6-311G** MP2|4-31G**. Corresponds to reaction A. [e] ΔE° (anh) + ΔE° (solv) Tomasi's SCRF, with the dielectric constant of water.

($E^{assoc} = -78.8$ kJ/mol and $\Delta E^{solv} = -95.9$ kJ/mol) and AMI4 ($E^{assoc} = -72.2$ kJ/mol and $\Delta E^{solv} = -98.2$ kJ/mol). However, it must be mentioned that the ab initio procedure for isolated molecules in a reaction field favors these tautomers much more and differentiates the others among themselves.

Isomerization of *neutral species* is described by equilibria A and B. Table 3 is illustrative. A first approach by ΔH° and ΔG°, according eqns 8, 19, and 20, gives that *tautomerizations to any imine isomer appear nonfavored for neutral species either in gas phase or in water*. In other words, this approach predicts an abundance of neutral AMF diamine, either as an isolated molecule or in water solution. This is in agreement with NMR results in water (see above). Ab initio results present a qualitative agreement with these calculations in the case of isolated molecules, although SCRF hydration reverses the trend to favor nonconjugated imine species such as AMI2B. It must be considered that this method for solvation effects does not explicitly take into account the protic character of the solvent but only its dielectric constant. Therefore, this result points to NMR experimental evidence in deuterated dimethyl sulfoxide, which shows the clear presence of a nonconjugated form, as AMI2B could be.
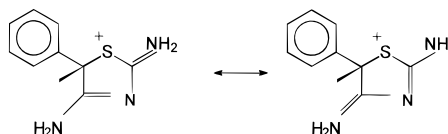
(c) Protonation. Protonation is described by reactions C and D, for gas-phase and solvated processes, respectively. According to these, and taking into account that we are dealing with five tautomers presenting four protonation sites each, we can afford up to 100 different reactions. All of them were calculated in the case of MMH exploration, and detailed results are available upon request. Table 4 is limited to showing the reactions of those corresponding to protonation of AMF, as a predominant species in the raw basic or neutral media (see Table 3). An interesting product of protonation is the C5 saturated monoimine 2B, when it is protonated in N2 and the one in 4 when it is protonated in N4. They are equivalent and fake a diamine protonated in C5. The molecular formula is displayed in Figure 3 and we designate it AMI2B(H2)-4(H4)⁺.

Ab initio models predict different products with respect to semiempirical calculations for the reaction in the gas phase. While the PM3 Hamiltonian predicts more or less the same preferences for protonation in diamines N(3), N(4), and the symmetric "monoimine", ab initio calculations predict AMI2B-(H2)-4(H4)⁺ as the largely preferred protonated structure. Let us point out that the order of magnitude of calculated energies in solution is more near to experimental conditions of equilibria than the very high values appearing for gas-phase reactions.

Table 4. Calculated Most Probable Tautomers after Protonation of AMF[a]

X	Y	PM3 $\Delta H°$(anh)[b]	MMH $\Delta H°$(hydr)[c]	MMH $\Delta G°$(hydr)[c]	SCF MP2 $\Delta E°$(anh)[e]	SCF MP2 $\Delta E°$(solv)[f]
AMF	AMF(H3)$^+$	−261.1	−111.9[d]	−83.9[d]	−247.2	−60.1
AMF	AMF(H4)$^+$	−263.5	−109.3[d]	−83.8[d]	−224.0	−62.4
AMF	AMI2B(H2)-4(H4)$^+$	−264.5	−95.2	−67.2	−298.0	−123.1
AMF	AMI2A(H4)$^+$	−203.51	14.24	12.84		
AMF	AMII(H4)$^+$	−216.23	24.78	26.23		
AMF	AMII(H2)$^+$	−220.87	30.03	30.12		
AMF	AMI2B(H3)$^+$	−216.23	33.90	34.36		
AMF	AMI4(H3)$^+$	−220.87	39.43	37.71		
AMF	AMF(H2)$^+$	−224.89	46.49	46.06		
AMF	AMI2A(H3)$^+$	−178.74	53.77	54.45		
AMF	AMI2B(H4)$^+$	−149.70	60.55	61.30		
AMF	AMI4(H2)$^+$	−152.26	65.52	63.71		
AMF	AMII(H3)$^+$	−146.61	85.99	84.26		
AMF	AMI2A(H1)$^+$	−174.72	94.29	92.36		
AMF	AMI2A(H2)$^+$	−172.26	101.65	100.22		
AMF	AMF(H1)$^+$	−172.26	105.03	104.72		
AMF	AMII(H1)$^+$	−121.04	116.57	117.42		
AMF	AMI2B(H1)$^+$	−143.76	123.99	122.98		
AMF	AMI4(H1)$^+$	−112.51	134.64	133.35		

[a] Energies in kJ/mol. The list is in ascending order of calculated free energies, $\Delta G°$, of hydrated species. Sites of protonation are denoted by *Hm*, *m* being the number of heavy atoms in thiazole ring with respect to S1. [b] MNDO-PM3 results for reaction C. [c] Reaction D. [d] Calculated on the basis of 45 cells, in place of 15, as used in other cases. [e] HF SCF 6-311G** MP2|4-31G** for reaction C. [f] $\Delta E°$ (anh) + $\Delta E°$ (SCRF). Tomasi's SCRF, with the dielectric constant of water.

Figure 3. Tautomeric species corresponding to the equivalent AMI2B-(H2)$^+$ and AMI4(H4)$^+$ monoimines.

It is clear that calculations by MMH and SCRF models, taking into account environmental effects, disagree. According to SCRF results, the AMI2B(H2)-4(H4)$^+$ tautomer is the most favored structure in a polar media having the dielectric constant of water. However, this form is nonsignificant in NMR spectra when recorded in heavy water, as discussed above. To the contrary, spectra in deuterated dimethyl sulfoxide, a polar and nonprotic solvent, show a clear preference for this interesting species, confirming the results of the SCRF calculations. MMH exploration success in water is due to the ability to take into account the effects of direct interactions with a protic solvent, in addition to those that originated in the polarity of the molecular environment.

(d) Equilibria in Acid Media. Isomerization reactions E and F in acid media imply 380 nontrivial alternatives, as is mentioned above, given five tautomeric forms and four protonation sites. Although all of them were calculated in our first approach, it was later shown that the only significant cases are conversions among protonated forms AMF(H3)$^+$, AMF(H4)$^+$, and AMI2B(H2)-4(H4)$^+$, which are preferred in solution according to the previous considerations. In this case where all

	ΔH^{PM3}	$\Delta H°$	$\Delta G°$	ΔE^{anh}	ΔE^{solv}
		MMH		SCRF	
AMF(H3)$^+$ → AMF(H4)$^+$	−2.4	2.6	−0.1	23.2	−2.3
AMF(H3)$^+$ → AMI2B(H2)-4(H4)$^+$	−3.4	16.7	16.7	−50.8	−63.0
AMF(H4)$^+$ → AMI2B(H2)-4(H4)$^+$	−1.0	14.1	16.6	−74.0	−60.7

energies are in kilojoules per mole. The above MMH values could also be calculated from those in Table 4 by using the Hess law of thermochemistry, as has been done in the case of

Table 5. Calculated Neutralizations of Protonated Amiphenazole and Its Most Probable Tautomer in the H*m* Position of the Thiazole Ring[a]

X	Y	$\Delta H°$(anh)[b]	$\Delta H°$(hydr)[c]	$\Delta G°$(hydr)[c]
AMI2B(H2)-4(H4)$^+$	AMF	−774.92	−328.68	−334.57
AMI2B(H2)-4(H4)$^+$	AMI2A	−757.68	−311.71	−318.73
AMF(H4)$^+$	AMF	−775.96	−314.62	−318.02
AMF(H3)$^+$	AMF	−778.39	−312.03	−317.96
AMI2B(H2)-4H(4)$^+$	AMI2A	−761.15	−311.81	−317.14
AMI2B(H2)-4(H4)$^+$	AMI2B	−725.92	−282.88	−298.94
AMF(H3)$^+$	AMI2B	−729.40	−282.97	−297.35
AMI2B(H2)-4(H4)$^+$	AMII	−732.45	−284.25	−290.58
AMF(H3)$^+$	AMII	−735.92	−284.35	−288.99
AMI2B(H2)-4(H4)$^+$	AMI4	−719.82	−278.16	−285.72
AMF(H3)$^+$	AMI4	−723.29	−278.25	−284.13
AMF(H4)$^+$	AMI2B	−726.97	−268.02	−283.20
AMF(H4)$^+$	AMII	−733.50	−269.40	−274.85
AMF(H4)$^+$	AMI4	−720.86	−263.30	−269.98

[a] All energies in kJ/mol. The list is in ascending order of calculated free energies $\Delta G°$ of hydrated species. [b] Reaction G. [c] Reaction H.

SCRF results. These data corroborate that the only model predicting the behavior of equilibria in water is MMH. Accurate SCRF calculations largely favors AMI2B(H2)-4(H4)$^+$, which must be the most preferred species in polar nonprotic solvents, as NMR results confirm.

(e) Neutralization. Table 5 shows the most favored cases of neutralization reactions according equilibria of eqns G and H, ordered by increasing ($G°$'s of a selection departing from the three most probable protonated forms in Table 4. Species with some possibilities of existence (AMF(H3)$^+$, AMF(H4)$^+$, and AMI2B(H2)-4(H4)$^+$) are neutralized, essentially, to AMF as it can be deduced from the leading values in Table 5 and by taking into account equilibria of neutral species in Table 3.

(f) Experimental and Theoretical UV Maximums. Figure 4 shows the experimental UV spectra of AMF in water at different pH values. As usually occurs in polar and protic media, the wide bands of this kind of spectra only allow a qualitative description. Wide bands in solution originate from several contributing factors, i.e., different rotovibrational, electronic, and molecular structures of each hydrated species having a significant population.
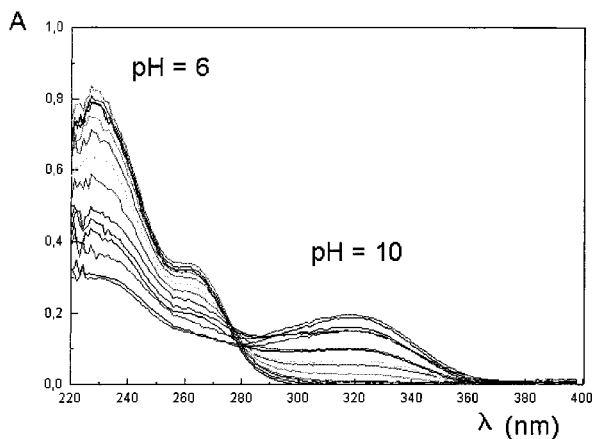
Figure 4. UV spectra of AMF in a Britton–Robinson buffer. Concentration was 0.04 mol/L from pH 6 to pH 10 (δpH = 0.4).

Table 6. Singlet Electronic Excitations[a]

	isolated molecules			hydrated molecules		
	ν (μm^{-1})	λ (nm)	f	ν (μm^{-1})	λ (nm)	f
Neutral Species (Higher pH Values)						
AMF[b]						
NDOL	3.92*	255	0.078	3.01*	332	0.096
	4.04**	248	0.221	3.46**	289	0.123
ZINDO/S	3.28**	305	0.570	3.40**	295	0.368
	3.99*	50	.219	3.91*	255	0.112
exp				3.1*	320	
				3.8 sh	260	
				4.3**	230	
Protonated Species (Lower pH Values)						
AMF(H3)$^+$						
NDOL	3.36*	297	0.050	2.99	335	0.054
	3.44**	291	0.067	3.80*	264	0.059
				4.14**	242	0.133
ZINDO/S	2.70*	371	0.219	2.89*	346	0.201
	4.39**	228	0.451	4.49**	223	0.542
AMF(H4)$^+$						
NDOL	3.74**	268	0.123	2.75**	363	0.124
	4.02*	249	0.122	3.57*	280	0.097
				3.65	274	0.055
ZINDO/S	3.56**	281	0.706	3.76**	266	0.527
	4.46*	224	0.187	4.55*	220	0.225
AMI2B(H2)-4(H4)$^+$						
NDOL	3.64**	275	0.115	2.75**	363	0.124
	3.93*	255	0.066	3.57*	280	0.097
				3.65	274	0.055
ZINDO/S	3.47*	288	0.040	3.67*	272	0.041
	4.44**	225	0.680	4.47**	224	0.698
exp				3.8*	265	
				4.4**	230	

[a] Only calculated excitations with $f > 0.01$ have been reported. Double-starred values correspond to the most intense bands, single-starred to secondary values, and nonstarred to the smallest values. Experimental shoulder bands are denoted by *sh*. [b] Hydrated AMF cell at the lowest MNDO-PM3 energy (see text).

In our case, the most important feature is that neutral species, appearing at higher pH values, show two flat bands around 320 and 230 nm, respectively. The sharper bands correspond to protonated species at low pH values, with peaks around 265 and 230 nm. Table 6 summarizes theoretical results for electron excitations of singlet states, in comparison with experimental UV maximums in solution. Theoretical calculations have been performed by two different procedures (NDOL[28] and ZINDO/S[32]) on the same supermolecules to test their respective responses in the case of large hydrated clusters.

Figure 5 presents the calculated spectra of AMF, both in gas phase (for the isolated molecule) and in water solution. In the
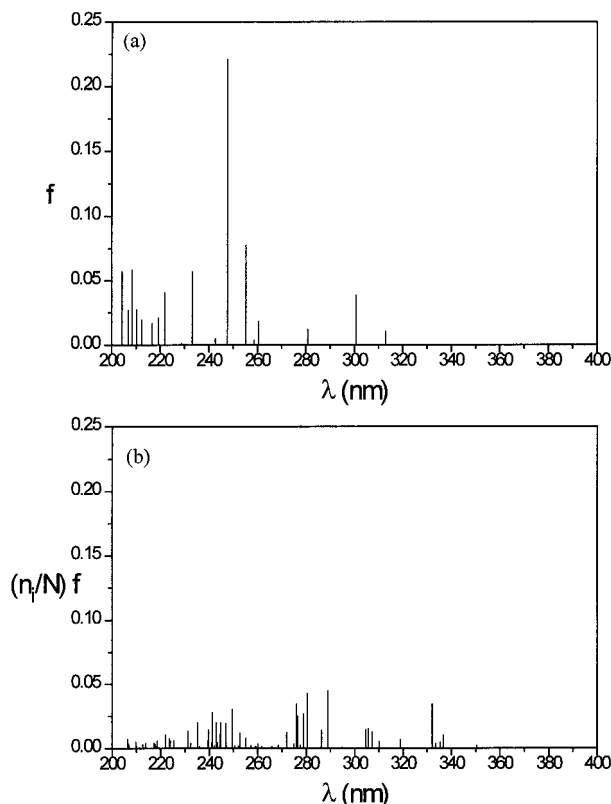

Figure 5. Calculated UV spectra of AMF in (a) gas phase and (b) with five water molecules by means of the NDOL procedure. f is the oscillator strength of each electronic transition of a wavelength λ (in nm). $(n_i/N)f$ is the normalized product of the Boltzmann population of ith cell times the oscillator strength. The four lowest energy supermolecules, up to a summed calculated population of 0.64, were selected in the hydrated case.

case of the solute–solvent supermolecule, four different cells presented low and similar association energies. Therefore, lines related to the oscillator strength f are shown with contributions proportional to their respective calculated Boltzmann populations, contrary to the single-cell values of f presented in all other theoretical spectra, as explained above. The dramatic change between NDOL calculations of the isolated and hydrated molecular spectra is shocking. A significant red shift due to bands of comparable intensity over 300 nm can be noted. In this case, it favors the agreement for prediction by this method, as shown in Table 6.

Figure 6 shows the calculated structures of both the isolated molecule and the lowest energy supermolecule. An interesting feature is the "bridge" of water molecules that are chained together and linking S1 with the substituted amine in C4 of the heterocyclic ring. It "crosses over" the surface of the phenyl ring. This is clearly a nonbonded and too ordered structure, and presumably, it is not representing an average behavior. Therefore, it can be inferred that, although the water MOs have no direct participation in the CI electronic transitions, they must be influencing their energy by perturbing significant Coulombic terms of truly interacting orbitals.

A theoretical analysis in the case of the NDOL method of the 248-nm band in the isolated molecule (the most intense) attributes it both to internal electronic transitions in the thiazole ring and charge transfers to excited orbitals in the benzene ring. In the supermolecule with the lowest energy, the first intense band appears at 332 nm and the most intense at 289 nm. Charge transfers between rings also influence the first one and the second is local in the thiazole ring. The water molecule bridge
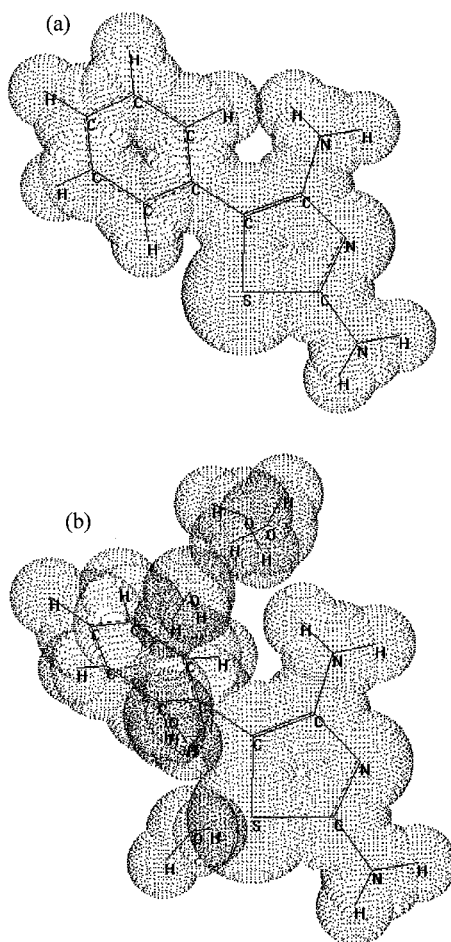
Figure 6. Outline of anhydrous (a) and hydrated (b) AMF in their respective minimal energy configurations.

Figure 7. Calculated UV spectra of AMF(H3)$^+$ in (a) gas phase and (b) with five water molecules by means of the NDOL procedure. f is the oscillator strength of each electronic transition of a wavelength λ (in nm). The hydrated species corresponds to the lowest energy supermolecule with a calculated population of 0.99.

between the amino group in C4 and sulfur atom apparently favors both transitions. ZINDO/S results are too far from the experimental values in this case.

In the case of protonated forms, for brevity's sake, we show here only figures corresponding to the MMH theoretically favored forms where protonation occurs in N3 and N4 sites. This is because they showed the best expectations after hydration in the case of MMH calculations from the energetic point of view (see Table 4). Supporting Information about all other forms can be obtained upon request to the authors. In any case, theoretical results for AMI2B(H2)-4(H4)$^+$ are also summarized in Table 6.

Figures 8 and 10 show the predicted hydrated clusters of AMF(H3)$^+$ and AMF(H4)$^+$, respectively, while Figures 7 and 9 show their corresponding calculated electronic transitions by the NDOL method. Table 6 shows results including the ZINDO/S method. The key experimental feature consisting in a blue shift upon protonation of amiphenazole is only clearly shown by ZINDO/S results of AMF(H4)$^+$, although this method failed to predict correct maximums in neutral hydrated AMF. However, given the predicted low intensity for the 335-nm NDOL theoretical band of protonated AMF(H3)$^+$ cluster, and the plausible agreement of the low-wavelength bands in this case, we can assume this result as acceptable, too. Such a band around 335 nm can really appear in the protonated form under the level of sensitivity of the spectra shown in Figure 4.

Figure 8 shows the theoretical shapes of the protonated species in N3, both the isolated molecule and the supermolecule of lowest energy. The main feature of the solvation shell here
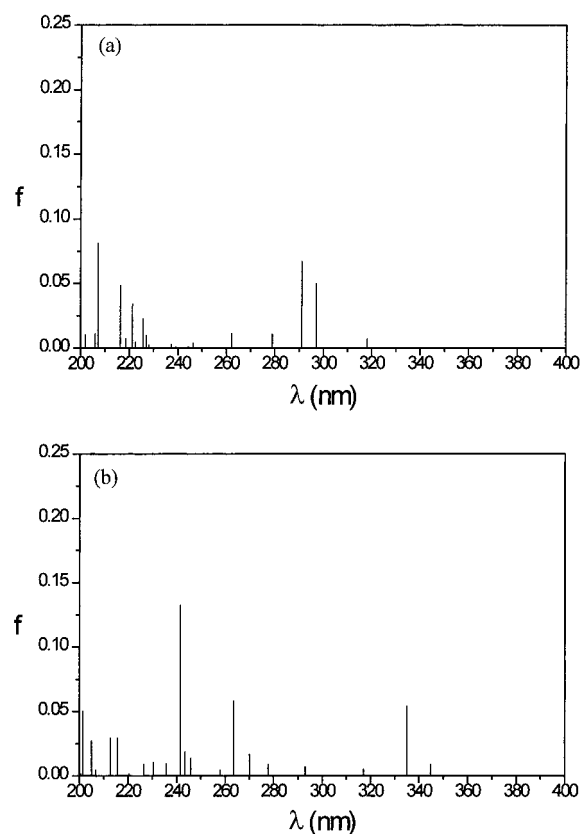
is that water surrounds both the protonated site in N3 and the amino group in C2. It can be observed that hydration at this level does not affect conjugation between both rings or their conjugated electron clouds. This fact can explain why the theoretical spectrum of this supermolecule very much resembles the one in Figure 5 corresponding to the isolated AMF, discounting the 335-nm band in this case. The perturbation due to the proton charge introduced here in N3 is neutralized by hydration, giving this similitude.

Figure 10 shows the theoretical shapes of the protonated species in N4, both the isolated molecule and the supermolecule of lowest energy. Although conjugation between both rings is low in either the anhydrous or hydrated molecule, it is apparent that the strong solvation of the protonated amino group shifts the intense band to the low-energy side of the spectrum as noted above.

Ionization Potentials and Electron Affinities of Predominant Species in Different Environments. Table 7 shows the calculated values for ionization potentials (according to Koopman's theorem) and electron affinities (taken as LUMO eigenvalues, with changed sign) of all neutral species in this complex equilibrium. PM3 values for electron affinities are not shown because this method used only ionization potentials and not LUMO eigenvalues for the basic parametrization. It must be pointed out that LUMO eigenvalues are nonconsistent in the case of closed-shell SCF calculations because of the absence of electron density in virtual orbitals to optimize their energy. However, as the NDOL method is a priori parametrized and it allows a certain predictive capacity from the qualitative point of view, we included the calculated data.
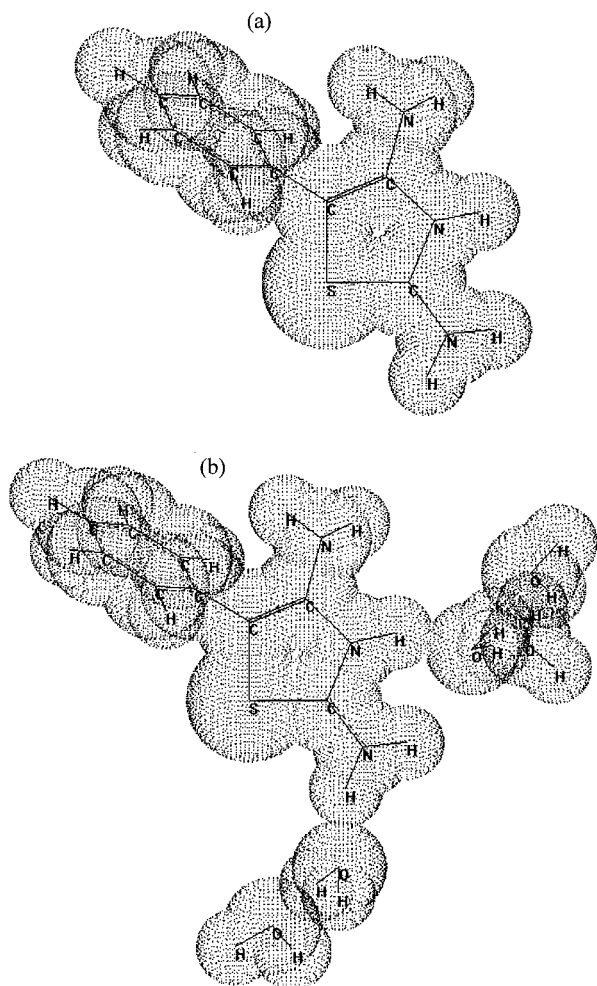
(a)

(b)

Figure 8. Outline of anhydrous (a) and hydrated (b) AMF(H3)⁺ in their respective minimal energy configurations.

Table 7. Koopman's Ionization Potentials and Electron Affinities of Neutral Species[a]

| | ionization potential (IP) | | | | electron affinity (EA) | |
| | PM3 | | NDOL | | NDOL | |
tautomer	anh	hydr	anh	hydr	anh	hydr
AMF	8.26	8.55	6.13	3.76	−1.17	−2.43
AMI2A	8.28	8.47	6.73	4.43	−0.63	−1.78
AMI2B	9.28	9.46	8.32	5.46	−0.51	−1.86
AMI4	9.16	9.30	7.84	5.35	−0.96	−2.23
AMII	9.35	9.56	8.39	5.34	−0.43	−1.93

[a] Calculated as IP $= -e^{HOMO}$ and EA $= -e^{LUMO}$. In electronvolts.

From the experimental point of view, it was impossible to determine potentiometric peaks for acid media in the case of protonated amiphenazole. Calculated ionization potentials of protonated molecules, 11.63 eV in the case of AMF(H3)⁺ and 11.92 eV in the case of AMF(H4)⁺ by PM3 method, fall very near to that of water, 12.32 eV, and it is an indication that the corresponding peaks must be overlapped by the solvent. It is an interesting conclusion of our calculations, and it is the reason that these values are absent from the table.

Our purpose to know theoretical qualitative preferences for acquiring (to be reduced) or leaving (to be oxidized) charge of these molecules under the action of an electrode potential. An overview shows that the PM3 method predicts slight increases of ionization potentials when the molecule is hydrated. The trend is reversed by the NDOL method, as could be deduced by simple intuition. Electron affinities also decrease upon hydration.
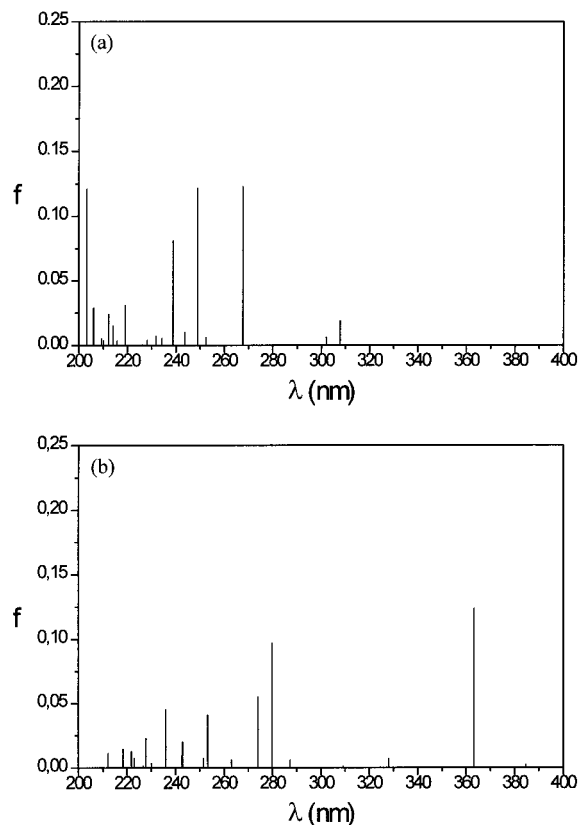

Figure 9. Calculated UV spectra of AMF(H4)⁺ in (a) gas phase and (b) with five water molecules by means of the NDOL procedure. f is the oscillator strength of each electronic transition of a wavelength λ (in nm). The hydrated species corresponds to the lowest energy supermolecule with a calculated population of 0.68.

Experimental evidence points to the oxidative behavior of AMF in solution. It can be deduced from the shape of the cyclic curve (I vs E) in Figure 11. If the electrode process oxidizes solute molecules, the most favored species is AMF, according NDOL, and AMI2A by PM3. It means that the most easily oxidized molecules are those with certain conjugation between the thiazole and phenyl rings. On the other hand, if molecules are reduced in the electrode process, the most favored molecule is AMI2A, with very similar results in the cases of AMI2B and AMII. In any case, the reduction of AMF in aqueous environments seems unlikely. This result could lead one to interpret the actual experimental process as oxidative.

Conclusions

The most interesting conclusion of this paper is the feasibility of an alternative way for calculating important features of chemical equilibria in solution by theoretical methods. It is clear that this is an important step toward a more extensive application of computational chemistry to understand problems in the experimental work of chemists.

From a very complete study of equilibria involving a system like 2,4-diamino-5-phenylthiazole, comprising five natural isomers each with four basic sites suitable for protonation, it remains that the diamine is most predominant in both acidic and basic media. As some monoimine species such as AMI2A can be present, even at room temperature, the electroanalytic signal can be affected to some extent.

Accurate SCRF theoretical models predict the behavior of equilibria in a polar environment. However, NMR results showed that they appear very influenced by direct interactions
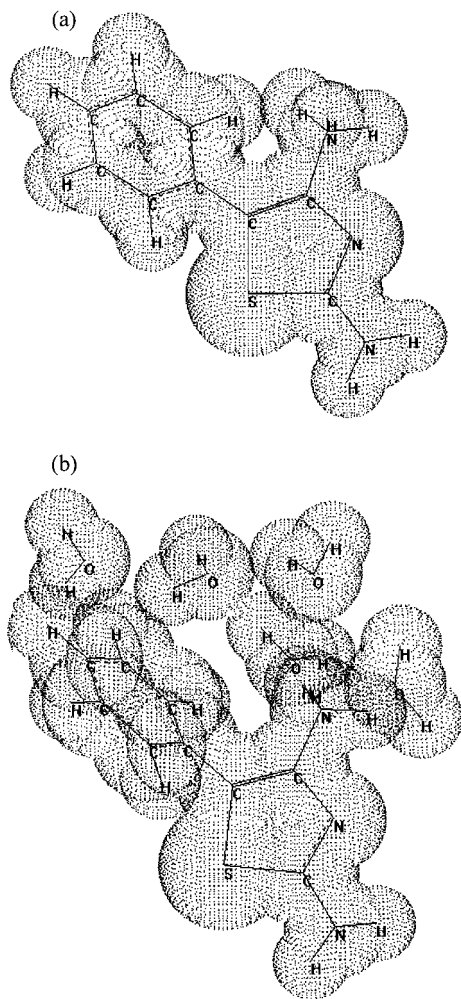
(a)

(b)

Figure 10. Outline of anhydrous (a) and hydrated (b) AMF(H4)$^+$ in their respective minimal energy configurations.
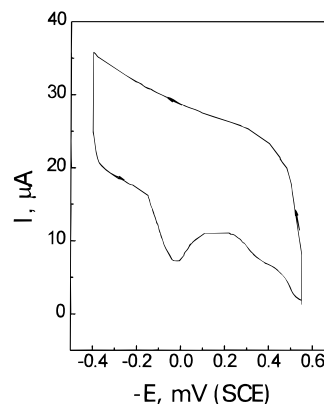

Figure 11. Cyclic voltamperogram (dc) of AMF (concentration 1×10^{-3} mol/L in NaOH 0.1 M) as obtained with a 3-mm^2 graphite paste electrode showing the oxidative peak. The potential was scanned from -0.4 to -0.55 V.

MOs have no direct participation in the CI electronic transitions, but they must be influencing their energy by perturbing significant properties of interacting orbitals. Previous studies are scarce[34] and use continuum models to reproduce environmental effects.

The classical UV spectra analysis and band assignment can be enriched with this approach. We found even the case of the diamine protonated in N3 had a pattern of electronic transitions very similar to anhydrous AMF. In this case, the conjugation between both the phenyl and thiazole rings was similar and solvation assumed influences of the proton associated to this position.

of protic solvent molecules with the solute, and this feature is better described by the MMH of hydrated supermolecules, as is outlined in this paper.

The solute for electroanalytic work must be a nonprotonated or neutral molecule, because of the similarity between HOMO eigenvalues of protonated molecules in solution and water itself. This result agrees very well with experimental evidence. Calculated results can also lead to the interpretation that the actual experimental process is oxidative.

From the study of theoretical electronic transitions, it can be concluded that they are strongly perturbed by solvation in these kinds of organic molecules. It can be inferred that the water

(34) Botrel, A.; le Beuze, A.; Jacques, P.; Strub, H. *J. Chem. Soc., Faraday Trans. 2*, **1984**, *80*, 1235.